Allosteric Control in *Limulus polyphemus* Hemocyanin: Functional Relevance of Interactions between Hexamers

Marius Brouwer*,‡ and Bjorn Serigstad§

Duke University Marine Laboratory/Marine Biomedical Center, Beaufort, North Carolina 28516, and Institute of Marine Research, Directorate of Fisheries, 5011 Bergen-Nordness, Norway

Received March 27, 1989; Revised Manuscript Received July 11, 1989

ABSTRACT: Hemocyanin of the horseshoe crab *Limulus polyphemus* is composed of 48 oxygen-binding subunits, which are arranged in eight hexameric building blocks. Allosteric interactions in this oligomeric protein have been examined by measurement of high-precision oxygen-equilibrium curves, using an automated Imai cell. Several models were compared in numerical analysis of the data. A number of conclusions can be drawn with confidence. (1) Oxygen binding by *Limulus* hemocyanin cannot satisfactorily be described by the two-state MWC model [Monod, J., Wyman, J., & Changeux, J. P. (1965) *J. Mol. Biol. 12*, 88–118] for allosteric transitions with either the hexamer or dodecamer as the allosteric unit. (2) Of the models tested, the data sets can be best described by an extended MWC model that allows for an equilibrium, within the 48-subunit ensemble, between cooperative hexamers and cooperative dodecamers. The model invokes T and R states for both hexamers (T6 and R6) and dodecamers (T12 and R12). Allosteric effectors modulate oxygen affinity and cooperativity by affecting the R to T equilibria within hexamers and dodecamers and by shifting the equilibria between hexamers and dodecamers. (3) The fitted model parameters show that under most conditions the intersubunit contacts within T-state hexamers are more constrained than those within T-state dodecamers. (4) The oxygen affinities of the hexameric and dodecameric R states are the same, but under all conditions examined the conformation of the fully oxygenated molecule is that of the dodecameric R state. (5) Between pH 7.4 and pH 8.5 the dodecameric T state has a higher affinity for oxygen than the hexameric T state, allowing for "T-state cooperativity". Outside this pH interval the oxygen affinities of the hexameric and dodecameric T states are the same. (6) The model is predictive and interpretive of the available structural data. The model parameters are well resolved within the nonlinear regression minimum obtained, and their pH dependence demonstrates that they reflect physical/chemical properties of the hemocyanin molecule.

Three classes of oxygen-carrying proteins occur in animals: hemoglobins, hemerythrins, and hemocyanins. The site of oxygen binding is entirely different in each: a single Fe(II) contained in a heme group in hemoglobins, two Fe(II) atoms bound by amino acid side chains in hemerythrins, and two Cu(I) atoms bound directly to side chains in hemocyanins. In hemerythrin oxygen is bound as a peroxide end-on to only one iron; in hemocyanin oxygen is bound as a μ-peroxo bridge to both coppers (Van Holde & Miller, 1982; Ellerton et al., 1983; Reem et al., 1987). These oxygen carriers are generally composed of multiple subunits, 4 for hemoglobin, 8 for hemerythrin, and 6–48 for arthropod hemocyanins, which allow for homotropic interactions between the oxygen-binding sites. Oxygen binding by hemoglobins and hemocyanins proceeds in a cooperative manner, but most hemerythrins bind oxygen noncooperatively, with the exception of the hemerythrins of some brachiopods (Richardson et al., 1983).

Homotropic and heterotropic interactions arise from conformational equilibria in which the conformers have different reactivities toward both active and non active site ligands. The respiratory proteins, having "spectrally active" binding sites on each of their interacting subunits, provide convenient model systems for analysis of allosteric mechanisms. Analysis of experimental data within the constraint of a model allows us to quantify homotropic and heterotropic effects and can provide insight into the molecular basis and mechanism involved. The most extensive and detailed application of theoretical models to experimental data has been done with tetrameric hemoglobin as a model protein. The two-state allosteric model of Monod, Wyman, and Changeux (MWC) (Monod et al., 1965), which postulates a conformational equilibrium between a state with low affinity for oxygen (T state) and a state with high affinity for oxygen (R state), has been found adequate to describe hemoglobin oxygenation under any single condition. However, the two-state model is inadequate to describe the effects of changing the concentrations of allosteric effectors. The presence of additional states has to be invoked, despite the observation of only two distinct structural states by X-ray crystallography (Minton & Imai, 1974; Edelstein, 1975; Imai, 1982; Straume & Johnson, 1988). Models that take into account fundamental postulates of both the two-state (MWC; Monod et al., 1965) and induced-fit (KNF; Koshland et al., 1966) allosteric models have been proposed (Di Cera et al., 1987).

Whereas hemoglobin is composed of four subunits, the quaternary structure of hemocyanins is more complex. The simplest arthropod hemocyanin is composed of six subunits arranged in two face to face stacked trimers that have a common 3-fold axis. The upper trimer is rotated 60° with respect to the lower one (Gaykema et al., 1984, 1986). More complex hemocyanins are built from two, four, or eight hexamers (Van Holde & Miller, 1982; Ellerton et al., 1983). This complexity raises the question of whether the interaction between hexamers has functional significance or whether the hexamers act as functionally independent units. To answer

‡ Duke University Marine Laboratory/Marine Biomedical Center.
§ Institute of Marine Research.

0006-2960/89/0428-8819$01.50/0

this question, we and others have studied oxygen binding by hemocyanins of increasing structural complexity. Oxygen binding by the relatively simple hexameric hemocyanin from the shrimp *Penaeus setiferus* can be described by a hybrid model that allows for the presence of one T and R state and an additional R3T3 hybrid state, indicating that the structural arrangement of the six subunits in two trimers may have functional implications (Brouwer et al., 1978). Similarly, oxygen binding by the dodecameric hemocyanin from the blue crab *Callinectes sapidus* and the 24-subunit hemocyanin from the ghost shrimp *Callianassa californiensis* can be described by the hybrid model. Both hemocyanins are composed of independently acting hexamers. Within each hexamer there are trimers which act semiindependently (Arisaka & Van Holde, 1979; Johnson et al., 1988). The binding of oxygen and carbon monoxide by the dodecameric hemocyanins from the mangrove crab *Scylla serrata* and the lobster *Homarus americanus* can be adequately analyzed with an extended MWC model including a third allosteric form (Richey et al., 1985). Interactions between hexamers seem not to occur. The very high cooperativity of the 24-subunit hemocyanin from the tarantula *Eurypelma californicum* can be explained by a "nested" model, in which the allosteric properties of two dodecameric allosteric units are dependent on the conformational state of the overall 24-mer (Decker et al., 1986, 1988; Robert et al., 1987). The so-called "cooperon" model, which combines features of the two-state and induced-fit models, has been found adequate in describing the cooperativity of ligand binding by the hemocyanin of the mollusc *Helix pomatia* (Coletta et al., 1986; Brunori et al., 1986).

Studies on oxygen binding by the 48-subunit hemocyanin from *Limulus polyphemus* show that the number of interacting sites, as analyzed within the context of the two-state model, can vary from about 6 to 10 (Brouwer et al., 1977, 1981, 1982, 1983). To further explore this phenomenon, we have investigated allosteric interactions in *L. polyphemus* hemocyanin by measurement of precise oxygen-binding curves under a wide variety of conditions. The nested and cooperon models can mathematically describe the binding data, but the fitted model parameters seem to be devoid of any physical meaning. A model based on the assumption that cooperative hexamers are in conformational equilibrium with cooperative dodecamers can quantify oxygen binding by *Limulus* hemocyanin under a wide variety of conditions. The best-fit model parameters are not merely numbers that best describe a set of binding data but reflect chemical/physical properties of the hemocyanin molecule. Analysis within the framework of this "Interacting Cooperative Units" or ICU model for allosteric transitions shows that allosteric effectors modulate oxygen affinity by affecting the (T6 + T12) → (R6 + R12) transition and affect cooperativity of oxygen binding by controlling the fraction of hexameric and dodecameric allosteric units that participate in the oxygen-binding process.

Theoretical Model for Oxygen Binding by *Limulus* Hemocyanin

Oxygen binding by *Limulus* hemocyanin cannot satisfactorily be described by the two-state model for allosteric transitions with either the hexamer or dodecamer as the allosteric unit. The number of interacting oxygen-binding sites (as analyzed within the framework of the two-state model) varies between 6 and 10, dependent upon pH and calcium concentration (see Discussion for details). This suggests the participation of discrete hexameric and dodecameric allosteric units in the oxygen-binding process. The relative abundance of both types of allosteric units is dependent on pH and calcium concentration. The oxygen-binding process can in this case be described by the following extension of the simple two-state model:

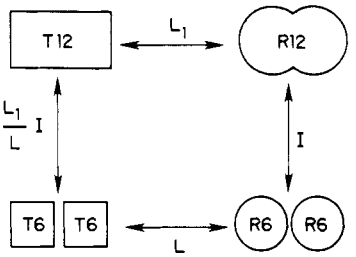

where T6T6 and R6R6 stand for dodecamers composed of two independent noninteracting hexamers in the T and R state, respectively, and T12 and R12 stand for dodecamers with 12 interacting oxygen-binding sites. It is assumed that the intrinsic oxygen-binding constants for T6 and T12 are the same. The same applies to the oxygen-binding constants of R6 and R12. In the absence of oxygen, the following conformational equilibria exist:

$$L = [T6]/[R6] \rightarrow [T6] = L[R6] \quad (1)$$

$$L_1 = [T12]/[R12] \quad (2)$$

$$I = [R12]/[R6R6] \rightarrow [R12] = 2I[R6] \quad (3)$$

The value of the fourth equilibrium constant [T12]/[T6T6] is given by

$$\frac{[T12]}{[T6T6]} = \frac{L_1 I}{L} \rightarrow [T12] = 2L_1 I[R6] \quad (4)$$

Since oxygen binding by the four conformational states is mutually exclusive, the total generating function, describing the oxygen binding by this macromolecular assembly, is given by the sum of the generating functions of the individual states (Hess & Szabo, 1979). Using the R6 state as a reference state, we obtain

$$P = (1 + \alpha)^n + L(1 + c\alpha)^n + 2I(1 + \alpha)^{2n} + 2L_1 I(1 + c\alpha)^{2n} \quad (5)$$

where $n = 6$, $\alpha = [O_2]/K_R$, $c = K_R/K_T$, and K_R and K_T are the oxygen dissociation constants of the R and T state. The restriction that the oxygen affinities of T6 and T12 (and those of R6 and R12) are the same can be easily released. For example, if the affinities of T6 and T12 are assumed to be different, but those of R6 and R12 are equal, then the values for c in the second and fourth terms of the binding polynomial become $c_1 = K_R/K_{T6}$ and $c_2 = K_R/K_{T12}$.

The saturation function $\bar{Y}$ can be obtained from the binding polynomial, with the following relationship (Heck, 1971; Hess & Szabo, 1979):

$$\bar{Y} = \frac{1}{n}\frac{\alpha}{P}\frac{dP}{d\alpha} \quad (6)$$

with $n = 6$ for the first two terms in eq 5 and $n = 12$ for the last two terms.

$$\bar{Y} = [\alpha(1 + \alpha)^{n-1} + Lc\alpha(1 + c\alpha)^{n-1} + 2I\alpha(1 + \alpha)^{2n-1} + 2L_1 Ic\alpha(1 + c\alpha)^{2n-1}]/[(1 + \alpha)^n + L(1 + c\alpha)^n + 2I(1 + \alpha)^{2n} + 2L_1 I(1 + c\alpha)^{2n}] \quad (7)$$

$$ABS = \bar{Y}(AMAX - AMIN) + AMIN \quad (8)$$

where ABS is the measured absorbance and AMAX and AMIN are the absorbances of the fully oxygenated and de-

oxygenated protein. If $I = 0$ or $I \rightarrow \infty$, eq 7 becomes the saturation function for the simple two-state model with 6 and 12 interacting sites, respectively. Taking D to be the denominator of eq 7

$$\bar{Y}_{\text{hexamer}} = [\alpha(1 + \alpha)^{n-1} + Lc\alpha(1 + c\alpha)^{n-1}]/D \quad (9)$$

$$\bar{Y}_{\text{dodecamer}} = [2I\alpha(1 + \alpha)^{2n-1} + 2L_1Ic\alpha(1 + c\alpha)^{2n-1}]/D \quad (10)$$

The fraction of molecules in the R6, T6, R12, and T12 states is given by

$$\text{R6} = (1 + \alpha)^n/D \quad (11)$$

$$\text{T6} = L(1 + c\alpha)^n/D \quad (12)$$

$$\text{R12} = 2I(1 + \alpha)^{2n}/D \quad (13)$$

$$\text{T12} = 2L_1I(1 + c\alpha)^{2n}/D \quad (14)$$

Hill plots are calculated with

$$\bar{Y}/(1 - \bar{Y}) = [\alpha(1 + \alpha)^{n-1} + Lc\alpha(1 + c\alpha)^{n-1} + 2I\alpha(1 + \alpha)^{2n-1} + 2L_1Ic\alpha(1 + c\alpha)^{2n-1}]/[(1 + \alpha)^{n-1} + L(1 + c\alpha)^{n-1} + 2I(1 + \alpha)^{2n-1} + 2L_1I(1 + c\alpha)^{2n-1}] \quad (15)$$

Materials and Methods

Limulus hemocyanin was prepared and purified as described previously (Brouwer et al., 1977; Brenowitz et al., 1981). Samples were in 50 mM tris(hydroxymethyl)aminomethane (Tris) containing 10 mM $CaCl_2$ (unless stated otherwise) made up to ionic strength 0.1 with NaCl (Bates, 1973).

Measurements of Oxygen-Equilibrium Curves and Numerical Analysis of the Experimental Data. Precise and complete oxygen-binding curves were determined in a temperature-controlled Imai apparatus, fitted with movable quartz windows for light transmission and an oxygen electrode for p_{O_2} measurements. The data acquisition process and the flow of gas (N_2, O_2, and air) through the cell are computer controlled. The 255 data points [p_{O_2} and absorbance (A)] collected with the Imai apparatus are analyzed with the program PRIMA (Johnson, 1984). The first processing involves deriving the fractional saturation according to $Y = (A - \text{AMIN})/(\text{AMAX} - \text{AMIN})$. An estimate of AMAX is obtained by fitting a polynomial of $1/p_{O_2}$ to the top 2% of the range of the absorbance data and extrapolation to the zero value of $1/p_{O_2}$ (infinite p_{O_2}). AMIN is obtained by fitting a polynomial of p_{O_2} to the bottom 2% of the absorbance values and extrapolation to $p_{O_2} = 0$. Next the PRIMA program calculates estimates of the parameters used to describe the oxygen-equilibrium curve (Monod et al., 1965; Brouwer et al., 1978). Finally, the program writes out a file of the smoothed absorbance and p_{O_2} data, together with an estimate of the standard error of the absorbance data calculated according to the method of Imai (1982). These estimates are used to weigh the data during the nonlinear regression analysis. This file and the estimates of the model parameters are used as input in the program NONLIN (Johnson et al., 1981; Turner et al., 1981), which fits the absorbance data to model saturation functions by means of a nonlinear least-squares regression procedure. The fitted model parameters obtained by NONLIN and the data file were then used as input in the program MINSQ (Micromath, Scientific Software), which allowed for graphical representation of the measured data and calculated functions. The final model parameters calculated by the MINSQ program are reported in this paper.

The statistical significance of the improvement in fit obtained by including the p_{50}s of the T6, R6, T12, and R12 states as floating parameters in the model equation (eq 7) was tested by use of the criterion of Mannervik (1982). The sums of the squared residuals for the original and extended models are compared by calculating the quotient

$$(\text{SRS}_o - \text{SRS}_e)(n - p_e)/(p_e - p_o)\text{SRS}_e \quad (16)$$

where n is the number of data points and p_o and p_e are the number of parameters in the original and extended model, which includes the absorbances in the presence and absence of oxygen as floatable parameters. The sum of the squared residuals for the two models is SRS_o and SRS_e. If the quotient (16) is greater than the F statistic $F(p_e - p_o, n - p_e)$, then the extension of the original model is warranted. For comparison of models that are not simple extensions of each other but are essentially different (see Discussion), we calculated

$$\frac{\text{SRS}_o/(n - p_o)}{\text{SRS}_e/(n - p_e)} \quad (17)$$

If this quotient is greater than 1.5, the model with the higher variance is rejected (Mannervik, 1982).

Analytical ultracentrifugation was used to ascertain that *Limulus* hemocyanin was in its undissociated aggregation state under the experimental conditions used (Brouwer et al., 1981).

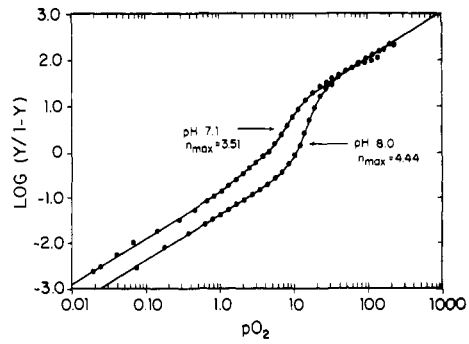

FIGURE 1: Effect of pH on Hill plots of the oxygen equilibria of *L. polyphemus* hemocyanin in 50 mM Tris containing 10 mM $CaCl_2$, ionic strength 0.1. Solid lines drawn through the experimental data points were calculated with eq 15 and the best-fit model parameters listed in Table I.

Results

Allosteric Effects of Protons: Bohr Effect. Both the affinity for oxygen and the cooperativity of oxygen binding by *Limulus* hemocyanin are dependent on the pH. The p_{50} values, i.e., the partial pressure of oxygen required for half-saturation of hemocyanin, and the slope of the Hill plots of oxygen binding increase in the pH interval from pH 7.1 to pH 8.8 (Figure 1 and Table I). Above pH 8.8 the value of both parameters decreases. The p_{50}s of the R6 and R12 states are only marginally affected by pH (Figure 1 and Table I). In contrast, the p_{50}s of the T6 and T12 states are strongly affected by pH, as evidenced by the shift of the deoxy asymptotes of the Hill plots presented in Figure 1. The allosteric equilibrium constants, describing the equilibria between the hexameric R and T states and the dodecameric R and T states, show similar dependencies on the pH (Figure 2A,B). Both L (T6/R6) and L_1 (T12/R12) show maximum values around pH 8. The observed pH dependencies demonstrate that two classes of allosteric proton-binding sites are present on the hexameric and dodecameric allosteric units, with pK values around 7.5 and 8.7, respectively. The first class of sites stabilizes the T6 and T12 states, whereas the second class stabilizes the R6 and R12 states. The equilibrium between the R6 and R12 states

Table I: Effect of pH, Calcium, and NaCl on the Allosteric Parameters of the ICU Model Describing Oxygen Binding by *L. polyphemus* Hemocyanin

pH	Ca^{2+} (mM)	L (T6/R6)	L_1 (T12/R12)	I (R12/R6R6)	$L_1(I/L)$ (T12/T6T6)	p_{50} T6 state	p_{50} T12 state	p_{50} R6 and R12 states	p_{50} obsd	n_{max}
7.1	10	992 ± 503	(1.033 ± 0.447)E08	(2.423 ± 0.640)E-06	0.255	8.43 ± 0.28		0.92 ± 0.04	4.39	3.51
7.4	10	(1.759 ± 0.747)E05	(1.244 ± 0.407)E10	(3.235 ± 0.538)E-07	0.0229	17.08 ± 0.41	7.42 ± 0.44	0.58 ± 0.03	5.21	3.35
7.4	10	(1.546 ± 0.703)E05	(6.418 ± 2.350)E09	(3.972 ± 0.722)E-07	0.0165	16.08 ± 0.35	7.23 ± 0.44	0.61 ± 0.03	5.30	3.19
7.5	10	(4.174 ± 1.637)E05	(7.632 ± 2.425)E09	(4.308 ± 0.966)E-07	0.0079	16.27 ± 0.28	7.33 ± 0.33	0.60 ± 0.03	5.57	3.55
7.6	10	(1.368 ± 0.704)E05	(9.840 ± 3.598)E09	(3.732 ± 0.938)E-07	0.0269	18.98 ± 0.66	10.55 ± 1.19	0.74 ± 0.05	6.22	3.69
7.6	10	(1.011 ± 0.612)E05	(8.319 ± 3.900)E09	(2.933 ± 0.936)E-07	0.0241	18.17 ± 0.69	11.11 ± 1.76	0.78 ± 0.06	6.31	3.56
7.6	10	(2.611 ± 0.910)E05	(1.163 ± 0.348)E10	(2.441 ± 0.491)E-07	0.0109	18.18 ± 0.35	9.15 ± 0.56	0.69 ± 0.03	6.30	3.56
7.8	10	(1.031 ± 0.321)E06	(1.853 ± 1.843)E10	(1.304 ± 0.527)E-07	0.0023	21.17 ± 0.39	11.83 ± 1.95	0.78 ± 0.04	8.44	4.71
8.0	10	(2.552 ± 1.742)E06	(4.514 ± 3.519)E10	(1.121 ± 1.194)E-07	0.0020	24.60 ± 0.55	12.24 ± 1.03	0.90 ± 0.06	10.97	3.99
8.0	10	(1.365 ± 0.269)E06	(4.470 ± 1.183)E10	(2.339 ± 0.518)E-07	0.0077	24.15 ± 0.35	13.45 ± 0.65	0.81 ± 0.02	8.85	4.76
8.5	10	(1.409 ± 1.207)E06	(3.883 ± 0.771)E10	(1.650 ± 1.161)E-06	0.0455	21.92 ± 0.48	13.23 ± 0.46	0.89 ± 0.02	9.43	3.90
8.8	10	(1.476 ± 0.421)E05	(1.944 ± 1.524)E10	(4.235 ± 1.234)E-07	0.0056	21.21 ± 0.31		1.35 ± 0.08	12.24	3.98
8.8	10	(2.323 ± 0.323)E05	(1.119 ± 0.693)E10	(1.463 ± 0.241)E-07	0.0071	21.30 ± 0.26		1.36 ± 0.08	12.11	4.39
9.0	10	(4.880 ± 1.352)E04	(1.601 ± 1.503)E09	(7.630 ± 4.036)E-07	0.0250	18.54 ± 0.47		1.39 ± 0.15	9.91	3.40
9.6	10	(6.632 ± 2.808)E03	(5.068 ± 3.317)E07	(8.473 ± 3.407)E-06	0.0647	20.78 ± 0.44		2.06 ± 0.08	10.34	3.25
8.0	1	(4.914 ± 0.932)E03	(1.729 ± 1.440)E07	(5.162 ± 2.901)E-06	0.0182	14.04 ± 0.22		1.63 ± 0.06	7.51	2.88
8.0	5	(1.518 ± 0.294)E06	(1.458 ± 0.284)E10	(1.382 ± 0.244)E-07	0.0013	25.16 ± 0.28	16.46 ± 0.61	0.92 ± 0.02	10.84	4.44
8.0 (0.5 M NaCl)	10	(1.296 ± 0.421)E04	(2.363 ± 1.338)E10	(9.629 ± 3.005)E-08	0.1755	19.68 ± 0.30		1.41 ± 0.07	10.43	2.92

[a] The best-fit model parameters were obtained by fitting oxygen-equilibrium data to eq 7 by nonlinear regression. Hemocyanin was in 50 mM Tris buffer, $I = 0.1$.

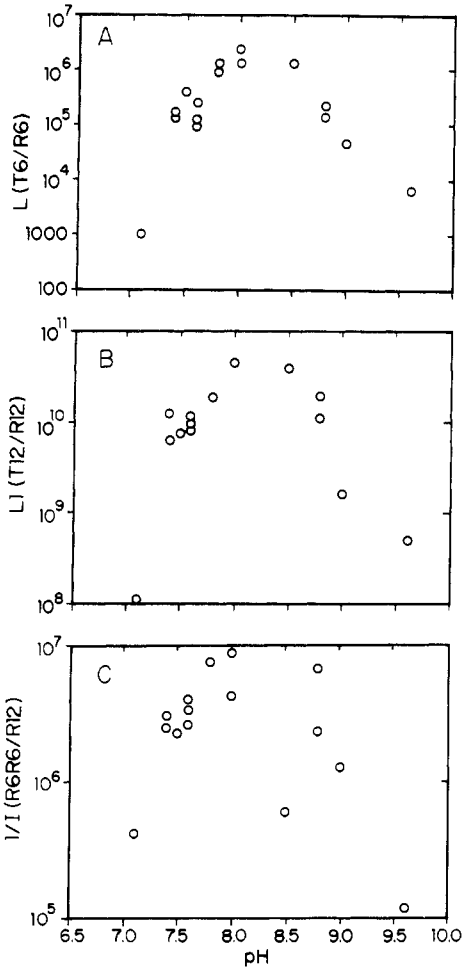

FIGURE 2: pH dependence of the allosteric equilibrium constants, as obtained by nonlinear regression analysis of the oxygen-equilibria data, using eq 7 as the model saturation function. (A) L is the equilibrium constant describing the conformational equilibrium between the unliganded hexameric T and R state (L = T6/R6). (B) L_1 is the equilibrium constant describing the conformational equilibrium between the unliganded dodecameric T and R states (L_1 = T12/R12). (C) $1/I$ is the equilibrium constant describing the conformational equilibrium between the unliganded hexameric and dodecameric R states ($1/I$ = R6R6/R12).

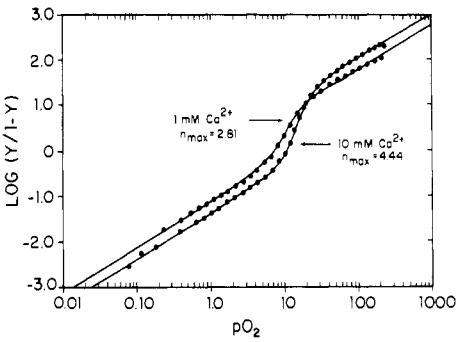

FIGURE 3: Effect of calcium on Hill plots of the oxygen equilibria of *L. polyphemus* hemocyanin in 50 mM Tris buffer, pH 8.0, ionic strength 0.1. Solid lines through the experimental data points were calculated with eq 15 and the best-fit model parameters listed in Table I.

shows a similar pH dependency as the equilibria between the T and R states (Figure 2C). The same applies to the pH dependency of the equilibrium between T6 and T12 (see Table I). This suggests that the proton-binding sites which control the T ↔ R equilibria, also control the hexamer ↔ dodecamer equilibria.

Allosteric Effects of Calcium. Calcium has multiple effects on the oxygen-binding parameters of *Limulus* hemocyanin at pH 8.0. First of all, calcium (1 → 5 mM) increases both the p_{50} value and cooperativity of oxygen binding (Figure 3 and Table I). Increases in calcium concentration above 5 mM have no effect on these parameters. In addition, calcium increases the oxygen affinity of the R state but decreases the affinity of the T state (Figure 3). At 1 mM calcium, the T6 state is favored over the R6 state by 4.95 kcal/mol, and T12 is favored over R12 by 9.70 kcal/mol. At 5 mM calcium these values increase to 8.28 and 13.62 kcal/mol, respectively (Table I). In addition to stabilizing the T6 and T12 states with respect to the R6 and R12 states, calcium also stabilizes the hexameric allosteric unit with respect to the dodecameric allosteric unit. For example, at 1 mM calcium R6 and T6 are favored over R12 and T12 by 7.08 and 2.33 kcal/mol, respectively. At 5 mM calcium these favorable interactions have increased to 9.19 and 3.86 kcal/mol (Table I). How these complex interactions affect the cooperativity of oxygen binding will be addressed under Discussion.

Allosteric Effects of Chloride. The main effect of NaCl on oxygen binding by *Limulus* hemocyanin is expressed in a decrease of the cooperativity of the oxygen-binding process

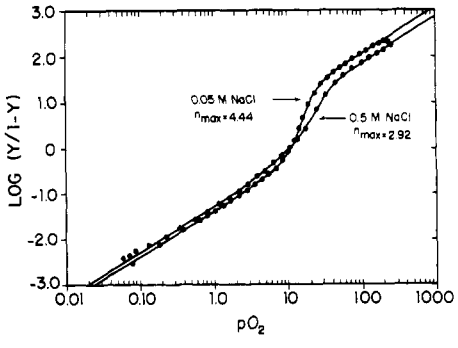

FIGURE 4: Effect of chloride on Hill plots of the oxygen equilibria of *L. polyphemus* hemocyanin in 50 mM Tris buffer, pH 8.0. Solid lines through the experimental data points were calculated with eq 15 and the best-fit model parameters listed in Table I.

(Figure 4, Table I). We have previously shown that this phenomenon is due to the interaction of chloride with hemocyanin (Brouwer et al., 1977). Chloride does not have an appreciable effect on the equilibria between the T12 and R12 states and the R6 and R12 states. Chloride does however have a strong effect on the equilibria between the T6 and R6 and between the T6 and T12 states. Addition of 0.5 M NaCl at pH 8.0, 10 mM $CaCl_2$, facilitates the T6 $\rightarrow$ R6 transition by approximately 3 kcal/mol and the T6 $\rightarrow$ T12 transition by approximately 2.5 kcal/mol (Table I).

Discussion

The hemocyanin of the horseshoe crab *L. polyphemus* is composed of 48 oxygen-binding subunits, which are arranged in eight hexameric building blocks (Lamy et al., 1982, 1983). The oxygen-binding data presented in this paper cannot adequately be described by the simple two-state model for allosteric transitions. When the number of interacting oxygen-binding sites (n) in the saturation function, which describes the oxygen-binding process within the framework of this model, is treated as a floatable parameter during the least-squares minimization procedure, the values of n converged upon are 5.28 (pH 7.1, 10 mM Ca), 5.85 (pH 7.4, 10 mM Ca), 6.18 (pH 7.5, 10 mM Ca), 7.72 (pH 8, 10 mM Ca), 6.62 (pH 8, 1 mM Ca), 5.57 (pH 8, 10 mM Ca, 0.5 M NaCl), 8.04 (pH 8.5, 10 mM Ca), 8.63 (pH 9, 10 mM Ca), and 9.6 (pH 9.6, 10 mM Ca). The number of interacting sites increases with pH and calcium concentration but decreases in the presence of NaCl. These observations suggest that allosteric interactions between *Limulus*' hexameric building blocks occur and that these interactions can be modulated by protons, calcium, and chloride ions.

Two models, which allow for such "higher order" reactions to occur, have recently been developed as extensions of the simple two-state model. The first model is based on the concept of nested allosteric interactions (Decker et al., 1986, 1988; Robert et al., 1987). The second, so-called cooperon model, is based on features of both the two-state and induced-fit models (Coletta et al., 1986; Brunori et al., 1986). In the concept of nesting there are two overall quaternary states, R and T, as in the classical allosteric formulation of the MWC model (Monod et al., 1965). Nested within the overall R state are two substates called Rr and Rt. Similarly within the overall T state there are two substates called Tr and Tt. Let us assume that *Limulus* hemocyanin is composed of MWC hexameric units which are nested inside a higher level (dodecameric) assembly, which can occupy either of two alternative quaternary conformations (R and T). The binding polynomial describing ligand binding to this macromolecular assembly is given by

$$P = A[B(1 + K_{Rr}x)^6 + C(1 + K_{Rt}x)^6]^2 + D[E(1 + K_{Tr}x)^6 + F(1 + K_{Tt}x)^6]^2 \quad (18)$$

where x is the activity of oxygen, $A = 1/(1 + L)$ is mole fraction of dodecamers in the R12 state ($L = T/R$), $D = L/(1 + L)$ is mole fraction of dodecamers in the T12 state, $B = 1/1 + l_R$ is mole fraction of hexamers in the Rr state (l_R is the equilibrium constant for the reaction r $\rightarrow$ t of the hexamer nested in the R overall conformation), $C = l_R/(1 + l_R)$ is mole fraction of hexamers in the Rt state, $E = l_T/(1 + l_T)$ is mole fraction of hexamers in the Tr state (l_T is the equilibrium constant for the reaction r $\rightarrow$ t of the hexamer nested in the T overall conformation), and $F = l_T/(1 + l_T)$ is mole fraction of hexamers in the Tt state. All conformational equilibria are defined as applying in the absence of ligand. The K's are equilibrium constants for ligand binding to each allosteric state. The fact that each subbinding polynomial in eq 18 is squared reflects the hypothesis of the nested model that the two hexamers, nested within the dodecamer, bind oxygen identically and that they do not interact with each other. In other words, binding of oxygen by either hexamer is independent of the other. The exponent arises from the rule that the probability of two independent events is equal to the product of their individual probabilities. In the model proposed in this paper, we postulate four states. Binding of oxygen to these states is mutually exclusive. The probability of occurrence of one of several mutually exclusive events is equal to the sum of their individual probabilities. The generating function for our proposed model (eq 5) is therefore composed of the sum of four terms. The average amount of ligand bound per macromolecule may be obtained by taking the partial derivative of the logarithm of P with respect to the logarithm of the ligand activity (Wyman, 1964; Heck, 1971; Hess & Szabo, 1979). The fractional saturation with ligand is

$$Y = \frac{1}{n}\frac{x}{P}\frac{dP}{dx} \text{ with } n = 12 \quad (19)$$

$$dP/dx = 2A\{6BK_{Rr}(1 + K_{Rr}x)^5 + 6CK_{Rt}(1 + K_{Rt}x)^5\}\{B(1 + K_{Rr}x)^6 + C(1 + K_{Rt}x)^6\} + 2D\{6EK_{Tr}(1 + K_{Tr}x)^5 + 6FK_{Tt}(1 + K_{Tt}x)^5\}\{E(1 + K_{Tr}x)^6 + F(1 + K_{Tt}x)^6\} \quad (20)$$

Oxygen-binding data were fitted to eq 19 with L, l_R, l_T, K_{Rr}, K_{Rt}, K_{Tr}, K_{Tt}, AMAX, and AMIN as floating parameters. It was found that the sum of the squared residuals (SRS: difference between actual dependent variable and the fitted function) was much smaller for the fit obtained with the nested model than that with the two-state model. Using the criteria outlined by Mannervik (1982) and eq 17, the nested model was judged superior in quantifying the data.

A number of observations makes the validity of the nested model in describing all of the binding data questionable: (1) The standard deviation of the fitted model parameters is very large. K_{Tr} and/or l_T can, in some cases, have almost any value without affecting the accuracy of the fit. (2) The regression procedure showed, for some data sets, the presence of more than one minimum with comparable standard error. Such data sets can thus be described equally well by very different values of the model parameters. A similar problem was encountered by Decker et al. (1988) in applying the nested model to oxygen binding by *Eurypelma* hemocyanin. (3) The dependency of the model parameters on pH is completely random. This suggests that the parameters may be mathematically correct but are devoid of any physical meaning.

The second model that allows functional interactions to extend beyond the level of the hexamer is the cooperon model

proposed by Brunori and co-workers (Brunori et al., 1986; Coletta et al., 1986). This model combines some of the features of the two-state (Monod et al., 1965) and induced-fit (Koshland et al., 1966) models. The hemocyanin is taken to be partitioned into a number of noninteracting functional constellations, each one existing in two possible quaternary conformations (R and T). A functional constellation is organized in several subsets of sites (called cooperons), in which subunits interact according to an induced-fit mechanism. X-ray crystallography of the hexameric hemocyanin of *Panulirus interruptus* shows that the hexamer can be best described as a trimer of dimers (Gaykema et al., 1984, 1986). It has been speculated that these quasirigid dimers rotate with respect to each other upon the binding of oxygen to the hexamer, analogous to the rotation of the α–β dimers upon oxygenation of hemoglobin (Gaykema et al., 1986). Assuming that *Limulus* hemocyanin is composed of four dodecameric functional constellations, each containing six dimeric cooperons, the binding polynomial for the whole hemocyanin is

$$P = [L/(1 + L)(1 + 2K_T x + i_T K_T^2 x^2)^6 + 1/(1 + L) \times (1 + 2K_R x + i_R K_R^2 x^2)^6]^4 \quad (21)$$

where $L = T/R$ is the equilibrium constant for the unliganded T and R quaternary structures of the dodecameric functional constellation and K_T and K_R are the observed equilibrium constants for the binding of oxygen to the T and R states. i_T and i_R are interaction constants that allow for cooperativity without a quaternary transition, localized at the interface between the two subunits forming the cooperon (Brunori et al., 1986). The fractional saturation with oxygen can be calculated with eq 19, with $n = 48$.

$$Y = [LM_T(1 + 2K_T x + i_T K_T^2 x^2)^5 + M_R(1 + 2K_R x + i_R K_R^2 x^2)^5]/[L(1 + 2K_T x + i_T K_T^2 x^2)^6 + (1 + 2K_R x + i_R K_R^2 x^2)^6] \quad (22)$$

with $M_T = K_T x(1 + i_T K_T x)$ and $M_R = K_R x(1 + i_R K_R x)$. Oxygen-binding data were fitted to eq 22, with L, K_T, K_R, i_T, i_R, AMAX, and AMIN as floating parameters. The cooperon model was superior to the simple two-state model in describing the data but was found to suffer from the same shortcomings as the nested model. The errors associated with the model parameters, especially L, K_R, and i_R, were found to be unacceptably large, i.e., larger than the values of the calculated parameters.

Since existing models for allosteric transitions were found incapable of adequately describing oxygen binding by *Limulus* hemocyanin, we derived a model equation based on the simple assumption that two hexameric cooperative units are in a reversible, conformational equilibrium with a dodecameric allosteric unit (see theory section for derivation of saturation function). This so-called interacting cooperative units or ICU model can quantify oxygen binding by *Limulus* hemocyanin, under a wide variety of conditions (see Table I for conditions and values of model parameters). The accuracy of the model was judged to be satisfactory on the basis of the following criteria: (1) In most cases, the sum of the squared residuals of the fit is superior to that of the other models tested. For example, at pH 8.0, 5 mM Ca, the SRSs for the simple two-state model with $n = 6$, $n = 12$, or n = variable (8.83) are 1.9241×10^{-3}, 9.9797×10^{-4}, and 3.6293×10^{-4}, respectively. For the nested and cooperon models the sum of the squared residuals further decreases to 2.0179×10^{-4} and 1.1308×10^{-4}, respectively. The ICU model gives SRS = 3.660×10^{-5}. When the p_{50}s of the T6 and T12 states are treated as floating parameters, a final, minimum SRS of 1.598×10^{-5} is attained. By use of the SRS values and eq 17 (Mannervik, 1982), the ICU model was judged superior in quantifying the data. (2) The standard deviations of the best-fit estimate for each parameter attest to the uniqueness of the fit obtained for each data set. (3) The values of model parameters determined by regression analysis of data collected in different experiments, but under the same conditions, are in good agreement (Table I). (4) The pH dependence of the parameters (Figure 2), obtained from the fitting procedure, suggests that the pK values of the amino acid residues involved in the proton-induced variation of each parameter are the same. This demonstrates that the model parameters are not merely numbers that best describe a set of binding data, but reflect physical/chemical properties of the hemocyanin molecule that should be amenable to physical/chemical probes.

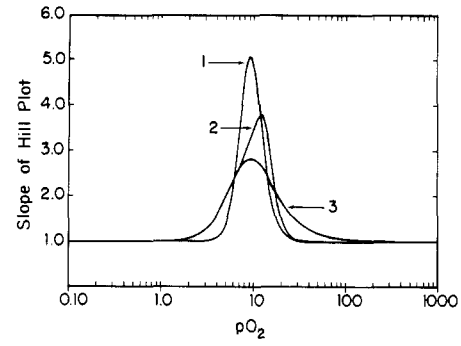

FIGURE 5: Degree of cooperativity (Hill slope) of oxygen binding by *L.* hemocyanin. The slope of the Hill plot was calculated with eq 7 and 23. The values for the model parameters were as follows: p_{50} of R state = 1 mmHg; p_{50} of T state = 20 mmHg; $L = 1 \times 10^5$ and $L_1 = 1 \times 10^{10}$. Curve 1: $I = 10^{60}$, dodecamers only. Curve 2: $I = 1 \times 10^{-7}$, cooperative hexamers in equilibrium with cooperative dodecamers. Curve 3: $I = 0$, hexamers only.

Inclusion of distinct p_{50} values for the T6 and T12 states in the model leads to results that, dependent on the pH, are statistically significantly better, according to the criteria described by Mannervik (1982), than results obtained with p_{50} values of T6 and T12 being equal. Between pH 7.4 and pH 8.5 the dodecameric T state has a higher affinity for oxygen than the hexameric T state (Table I). Since the fraction of molecules in the T6 state drastically decreases when the first oxygen molecules are bound, whereas the fraction of T12 increases (see below; Figure 6), this implies that oxygen binding to the T states is a cooperative process, a feature that our ICU model has in common with both the nested and the cooperon model (Brunori, 1986; Decker et al., 1988). The p_{50} values for T6 and T12, reported in Table I, are pH dependent, which indicates that protons also affect the oxygen-binding properties of the T state via pH-induced changes in the tertiary conformation of the T subunits. Inclusion of the p_{50} values of the R6 and R12 states in the model does not improve the accuracy of the fit. Moreover, the estimated values for p_{50} of the hypothetical R6 and R12 states are statistically the same. Oxygen binding to the R states is thus a noncooperative process. Similar observations have been made for oxygen binding by the R-state conformation of *Helix* and *Homarus* hemocyanin, analyzed within the framework of the cooperon model (Brunori et al., 1986).

Hill plots of oxygen binding by *Limulus* hemocyanin are generally characterized by three noticeable features: (1) asymmetry of the binding curves, (2) narrow p_{O_2} range over which the T $\rightarrow$ R transition occurs and extended T- and R-state asymptotes, and (3) moderate values of the Hill coefficients. We will first examine how these general properties may be explained by the ICU model, before proceeding to a

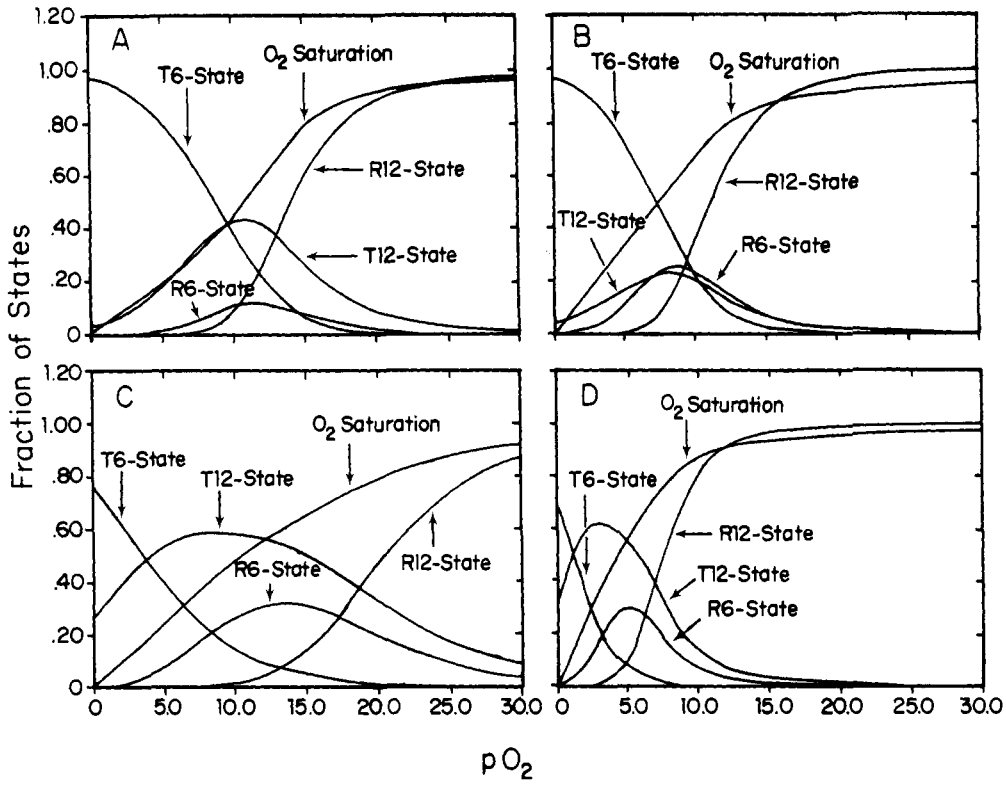

FIGURE 6: Fractional O_2 saturation and distribution of T6, T12, R6, and R12 states as a function of p_{O_2}. Saturation and state functions were calculated with eq 7 and 11–14 and the best-fit model parameters listed in Table I. (A) 50 mM Tris, 10 mM $CaCl_2$, pH 8.0. (B) 50 mM Tris, 1 mM $CaCl_2$, pH 8.0. (C) 50 mM Tris, 10 mM $CaCl_2$, 0.5 M NaCl, pH 8.0. (D) 50 mM Tris, 10 mM $CaCl_2$, pH 7.1.

more detailed interpretation of the oxygen-binding data. Figure 5 presents a graph of the slope of simulated Hill plots of oxygen binding as a function of p_{O_2}. The slope was calculated with

$$n = \frac{\mathrm{d} \ln [\bar{Y}/(1 - \bar{Y})]}{\mathrm{d} \ln \alpha} \qquad (23)$$

where $\bar{Y}$ is given by eq 7. The model parameter values used in the calculations are given in the figure legends. When $I = 0$, eq 7 becomes the saturation function of a MWC hexamer. The maximum slope of the Hill plot of oxygen binding by the hexamer is 2.838 and occurs at a p_{O_2} of 9.36 mmHg. The p_{50} is 7.60. The transition from the T state ($n = 1$ at low p_{O_2}) to the R state ($n = 1$ at high p_{O_2}) extends over a large p_{O_2} interval (Figure 5). Inclusion of the hexamer $\leftrightarrow$ dodecamer equilibrium ($I = 1.5 \times 10^{-7}$; see Table I) increases the maximum slope of the Hill plot to 3.949, which occurs at a p_{O_2} of 11.50 mmHg. The p_{50} is 7.71 mmHg. The T (T6 + T12) to R (R6 + R12) transition occurs over a much narrower p_{O_2} interval. At infinitely large values of I, eq 7 represents the saturation function of a MWC dodecamer. The maximum Hill coefficient for oxygen binding by the dodecamer ($I = 10^{60}$) is 5.084 and occurs at a p_{O_2} of 9.24 mmHg. The p_{50} is 8.10. The Hill plots of oxygen binding by the hexamer and dodecamer are slightly asymmetric, as reflected in the differences between the p_{O_2} at n_{max} and the p_{O_2} at half-saturation, which are 1.76 and 1.14 mmHg, respectively. Inclusion of the hexamer $\leftrightarrow$ dodecamer equilibrium increases this value to 3.37 mmHg, making the Hill plot much more asymmetric. The foregoing discussion shows how the inclusion of the hexamer $\leftrightarrow$ dodecamer equilibrium in the MWC allosteric model helps to describe the salient features of the oxygen-binding process by *Limulus* hemocyanin.

Allosteric effectors can modulate oxygen binding by *Limulus* hemocyanin by affecting the equilibria between the four conformational states. Since these equilibria are linked, it is difficult to explain observed changes in oxygen-binding behavior by simple inspection of the model parameters. A better understanding of how allosteric effectors accomplish their action can be obtained by calculating how they affect the distribution of the T6, T12, R6, and R12 states during the course of oxygenation and how they affect the partitioning of O_2 over the hexameric and dodecameric cooperative units that participate in the oxygenation process. The distribution of states shows a common pathway for the four data sets presented in Figure 6. Under deoxy conditions, only the T states are populated. Both protons and chloride stabilize the T12 state with respect to the T6 state. As oxygenation progresses, the fraction of hemocyanin molecules in the T6 state monotonically decreases to zero. Both the hexameric R state and dodecameric T state increase in concentration with increasing p_{O_2} and then pass through a maximum and subsequently fall off to zero. The fraction of dodecamers in the R-state conformation increases in a sigmoidal, cooperative manner with p_{O_2}, and the fully oxygenated molecule exists entirely in the R12-state conformation.

In the classical two-state model, the effect of allosteric effectors on the ligand affinity of the macromolecule is explained by assuming that the effector stabilizes either one of the two quaternary conformational states available to the macromolecule. The situation for the ICU model developed in this paper is more complex. A useful way of explaining the effect of allosteric effectors within the framework of this model is to relate effector concentration to the switchover point in the allosteric transition, which we define as the p_{O_2} where the concentration of the molecules in the T state equals that of the molecules in the R state, i.e., T6 + T12 = R6 + R12. The switchover point can be determined by plotting the sum of T6 + T12 and R6 + R12 against p_{O_2}. The p_{O_2} where the two graphs intersect constitutes the switchover point. At pH 8 + 10 mM Ca^{2+}, pH 8 + 1 mM Ca^{2+}, pH 8 + 10 mM Ca^{2+} + 0.5 M NaCl, and pH 7.1 + 10 mM Ca^2, the switchover in the

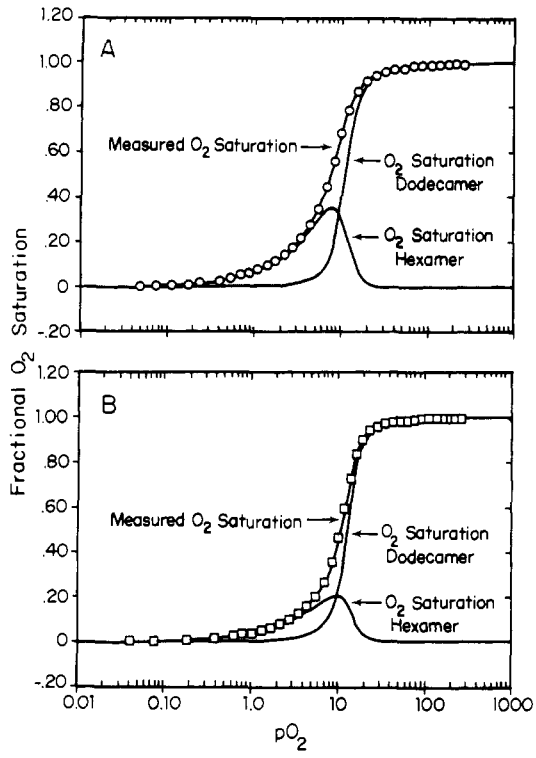

FIGURE 7: Oxygen-equilibrium curves of *Limulus* hemocyanin in 50 mM Tris, pH 8.0, with 1 mM $CaCl_2$ (A) and 10 mM $CaCl_2$ (B). The solid line through the experimental data was calculated with eq 7. The saturation of hexamers and dodecamers with oxygen was calculated with eq 9 and 10 and the best-fit model parameters listed in Table I.

allosteric transition occurs at p_{O_2} values of 13.3, 9.4, 16.2, and 6.0 mmHg respectively. The fractional O_2 saturation of hemocyanin under these conditions is very similar: $\bar{Y} = 0.676$, $\bar{Y} = 0.686$, $\bar{Y} = 0.629$, and $\bar{Y} = 0.640$. It is thus clear that calcium, chloride, and protons modulate the oxygen affinity of *Limulus* hemocyanin by inhibiting or facilitating the (T6 + T12) $\rightarrow$ (R6 + R12) transition.

At pH 8 + 10 mM Ca^{2+}, 24% of the molecules at the switchover point in the allosteric transition (p_{O_2} = 13.3 mmHg) occur in the hexameric allosteric conformation (T6 = 0.14 and R6 = 0.10) and 76% in the dodecameric allosteric conformation (T12 = 0.36 and R12 = 0.40). At the switchover point at pH 8 + 1 mM Ca^{2+} (p_{O_2} = 9.4 mmHg), the hexameric conformation comprises 53% (T6 = 0.28 and R6 = 0.25) of the total and the dodecamers 47% (T12 = 0.22 and R12 = 0.25). Calcium thus increases the fraction of dodecameric cooperative units at the allosteric switchover point, which in turn increases the cooperativity of oxygen binding. Chloride and protons, on the other hand, increase the fraction of cooperative hexameric units at the switchover point, which results in diminished cooperativity of oxygen binding. Panels A and B of Figure 7 display how the measured oxygen-binding curves of *Limulus* hemocyanin, at pH 8 + 10 mM Ca^{2+} and pH 8 + 1 mM Ca^{2+}, are composed of two saturation functions, which correspond to oxygen binding by the hexameric and dodecameric allosteric units. These theoretical binding curves have been calculated with eq 9 and 10 and the model parameters that are given in Table I. These figures clearly demonstrate that calcium inhibits the participation of the allosteric hexamers in the oxygen-binding process and hence promotes cooperativity of oxygen binding.

Cooperative oxygen binding by hemoglobin and *Limulus* hemocyanin is accompanied by changes in binding free energy and changes in the free energy of quaternary constraint (Mills et al., 1976; Brouwer et al., 1982). Stabilizing interactions, present in the constrained deoxy quaternary structure of *Limulus* hemocyanin, are abolished upon oxygenation (Brouwer et al., 1981). Here we will address the question of whether the transition from a hexameric to a dodecameric cooperative unit merely involves the doubling of the number of interacting oxygen-binding sites or also involves changes in the free energy of quaternary constraint. If, in the absence of such changes, the total change in free energy of quaternary constraint upon oxygenation of the hexamer is X kcal/6 mol of O_2, then the total change upon oxygenation of the dodecamer will be $2X$ kcal/12 mol of O_2. $X = -RT \ln L$ and $2X = -RT \ln L_1$, where L = T6/R6 and L_1 = T12/R12. From this it follows that $LL = L_1$. On the other hand, if the release of quaternary constraint per oxygen-binding step is greater for the dodecameric allosteric unit than for the hexamer, $L_1/LL > 1$. If the release per binding step is smaller, then $L_1/LL < 1$. The quotient L_1/LL can be calculated with the parameters listed in Table I. The standard deviation, SD, of L_1/LL was calculated according to SD of $(L_1/LL) = (L_1/LL)[((\text{SD of } L_1)/L_1)^2 + ((\text{SD of } L^2)/L^2)^2]^{1/2}$. The calculations indicate that L_1/LL is significantly less than 1 for all the data sets collected at 10 or 5 mM Ca^{2+}, between pH 7.4 and pH 8.8. This demonstrates that the average release of free energy of quaternary constraint per O_2-binding step is greater in the hexameric allosteric unit than in the dodecamer. This is not surprising in view of the observation that the oxygen affinity of the T6 state under these experimental conditions is lower than the O_2 affinity of the T12 state (Table I), which indicates that the T6 state is more constrained than the T12 state. At low pH (pH 7.1) and high salt (0.5 M NaCl), L_1/LL is significantly greater than 1. Under these conditions the T12 state seems to be more constrained than the T6 state. It seems therefore that the transition from the hexameric to dodecameric allosteric unit not only involves the doubling of the number of interacting oxygen-binding sites but also has a profound effect on the free energy of quaternary constraint of the T6 and T12 quaternary states.

In conclusion we may say that the ICU model described in this paper is consistent with the molecular architecture of the *Limulus* hemocyanin molecule. This 48-subunit polymer is composed of eight hexameric units, which are arranged in four dodecameric units (Lamy et al., 1982, 1983). The dodecamers, which are stable under very limited conditions, can bind oxygen in a cooperative manner (Brenowitz et al., 1984). The dodecamers cannot be dissociated into hexamers, attesting to the structural uniqueness of the dodecamer within the 48-mer (Johnson & Yphantis, 1978). The model is not only consistent with structural data but describes the binding data to high precision, and the values of the model parameters are well resolved within in the nonlinear regression minimum obtained (Table I). The model assumes that the oxygen affinities of the subunits within the polymer are the same, which seems at odds with the observation that the ligand-binding properties of the fractionated subunits are different (Sullivan et al., 1974; Bonaventura et al., 1974). We must keep in mind that the functional differences between the different subunits are small, except for subunits V and VI, which occur in small amounts (Sullivan et al., 1974). Moreover, the undissociated *Limulus* hemocyanin can be frozen in a noncooperative, low oxygen affinity conformation, which does not show any functional heterogeneity (Brouwer et al., 1977). In addition, there is a difference between the oxygen affinity of free subunits and that of subunits within the R state (Brouwer et al., 1981). These observations clearly suggest that the functional prop-

erties of the subunits change upon incorporation into the native 48-subunit macromolecule. Our proposed model must be ultimately tested by structural studies. To determine which subunits provide the functional coupling between the hexamers, we plan to study the oxygen-binding behavior of hemocyanin hybrids, in which subunits II and IV, which occur at the interhexamer interface (Lamy et al., 1982, 1983), have been replaced by Hg(II)-modified subunits, which have lost the ability to participate in cooperative interactions (Brouwer et al., 1983).

Registry No. O_2, 7782-44-7; Ca, 7440-70-2.

References

Arisaka, F., & Van Holde, K. E. (1979) *J. Mol. Biol. 134*, 41–73.

Bates, R. G. (1973) *Determination of pH, Theory and Practice*, Wiley, New York.

Bonaventura, C., Sullivan, B., Bonaventura, J., & Bourne, S. (1974) *Biochemistry 13*, 4784–4789.

Brenowitz, M., Bonaventura, C., Bonaventura, J., & Gianazza, E. (1981) *Arch. Biochem. Biophys. 210*, 748–761.

Brenowitz, M., Bonaventura, C., & Bonaventura, J. (1984) *Biochemistry 23*, 879–888.

Brouwer, M., Bonaventura, C., & Bonaventura, J. (1977) *Biochemistry 16*, 3897–3902.

Brouwer, M., Bonaventura, C., & Bonaventura, J. (1978) *Biochemistry 17*, 2148–2154.

Brouwer, M., Bonaventura, C., & Bonaventura, J. (1981) *Biochemistry 20*, 1842–1848.

Brouwer, M., Bonaventura, C., & Bonaventura, J. (1982) in *Physiology and Biology of Horseshoe Crabs: Studies on Normal and Environmentally Stressed Animals* (Bonaventura, J., Bonaventura, C., & Tesh, S., Eds.) pp 231–256, Alan R. Liss, New York.

Brouwer, M., Bonaventura, C., & Bonaventura, J. (1983) *Biochemistry 22*, 4713–4723.

Brunori, M., Coletta, M., & Di Cera, E. (1986) *Biophys. Chem. 23*, 215–222.

Coletta, M., Di Cera, E., & Brunori, M. (1986) in *Invertebrate Oxygen Carriers* (Linzen, B., Ed.) pp 375–381, Springer-Verlag, Berlin and Heidelberg.

Decker, H., Robert, C. H., & Gill, S. J. (1986) in *Invertebrate Oxygen Carriers* (Linzen, B., Ed.) pp 383–388, Springer-Verlag, Berlin and Heidelberg.

Decker, H., Conelly, P. R., Robert, C. H., & Gill, S. J. (1988) *Biochemistry 27*, 6901–6908.

Di Cera, E., Robert, C. H., & Gill, S. J. (1987) *Biochemistry 26*, 4003–4008.

Edelstein, S. J. (1975) *Annu. Rev. Biochem. 44*, 209–232.

Ellerton, D. H., Ellerton, N. F., & Robinson, H. A. (1983) *Prog. Biophys. Mol. Biol. 41*, 143–248.

Gaykema, W. P. J., Hol, W. G. J., Vereijken, J. M., Soeter, N. M., Bak, H. J., & Beintema, J. J. (1984) *Nature 309*, 23–29.

Gaykema, W. P. J., Volbeda, A., & Hol, W. G. J. (1986) *J. Mol. Biol. 187*, 255–275.

Heck, H. d'A. (1971) *J. Am. Chem. Soc. 93*, 23–29.

Hess, V. L., & Attilla, S. (1979) *J. Chem. Ed. 56*, 289–293.

Imai, K. (1982) *Allosteric Effects in Hemoglobin*, Cambridge University Press, New York.

Johnson, B. A. (1984) Allosteric Interactions of L-Lactate and Inorganic Ions with Structurally Distinct Crustacean Hemocyanins, Ph.D. Thesis, Duke University, Durham, NC.

Johnson, B. A., Bonaventura, C., & Bonaventura, J. (1988) *Biochemistry 27*, 1995–2001.

Johnson, M. L., & Yphantis, D. A. (1978) *Biochemistry 17*, 1448–1455.

Johnson, M. L., Correia, J. J., Yphantis, D. A., & Halvorson, H. R. (1981) *Biophys. J. 36*, 575–588.

Koshland, D. E., Nemethy, G., & Filmer, D. (1966) *Biochemistry 5*, 365–385.

Lamy, J., Sizaret, P. Y., Frank, J., Verschoor, A., Feldman, R., & Bonaventura, J. (1982) *Biochemistry 21*, 6825–6833.

Lamy, J., Lamy, J., Sizaret, P. Y., Billiald, P., Jolles, P., Jolles, J., Feldman, R. J., & Bonaventura, J. (1983) *Biochemistry 22*, 5573–5583.

Mannervik, B. (1982) *Methods Enzymol. 87*, 370–390.

Mills, F. C., Johnson, M. L., & Ackers, G. K. (1976) *Biochemistry 15*, 5350–5362.

Minton, A. P., & Imai, K. (1974) *Proc. Natl. Acad. Sci. U.S.A. 71*, 1418–1421.

Monod, J., Wyman, J., & Changeux, J. P. (1965) *J. Mol. Biol. 12*, 88–118.

Reem, R. C., & Solomon, E. I. (1987) *J. Am. Chem. Soc. 109*, 1216–1226.

Richardson, D. E., Reem, R. C., & Solomon, E. I. (1983) *J. Am. Chem. Soc. 105*, 7780–7781.

Richey, B., Decker, H., & Gill, S. J. (1985) *Biochemistry 24*, 109–117.

Robert, C. H., Decker, H., Richey, B., Gill, S. J., & Wyman, J. (1987) *Proc. Natl. Acad. Sci. U.S.A. 84*, 1891–1895.

Straume, M., & Johnson, M. L. (1988) *Biochemistry 27*, 1302–1310.

Sullivan, B., Bonaventura, J., & Bonaventura, C. (1974) *Proc. Natl. Acad. Sci. U.S.A. 71*, 2558–2562.

Turner, B. W., Pettigrew, D. W., & Ackers, G. K. (1981) *Methods Enzymol. 76*, 596–628.

Van Holde, K. E., & Miller, K. I. (1982) *Q. Rev. Biophys. 15*, 1–129.

Wyman, J. (1964) *Adv. Protein Chem. 19*, 223–286.